J. Biochem. 124, 1178-1187 (1998)

Mg^{2+} Binding and Catalytic Function of Sphingomyelinase from *Bacillus cereus*[1]

Shinobu Fujii,* Bunpei Inoue,* Hiroki Yamamoto,* Kenji Ogata,* Tomohiro Shinki,* Seiji Inoue,* Masahiro Tomita,† Hiro-omi Tamura,‡ Kikuo Tsukamoto,§ Hiroh Ikezawa,§ and Kiyoshi Ikeda*,[2]

*Department of Biochemistry, Osaka University of Pharmaceutical Sciences, Takatsuki, Osaka 569-1094; †Faculty of Engineering, Mie University, Tsu, Mie 514-8507; ‡Kyoritsu College of Pharmacy, Minato-ku, Tokyo 105-8512; and §Department of Microbial Chemistry, Faculty of Pharmaceutical Sciences, Nagoya City University, Nagoya, Aichi 467-8603

Received for publication, July 23, 1998

The modes of Mg^{2+} binding to SMase from *Bacillus cereus* were studied on the basis of the changes in the tryptophyl fluorescence intensity. This enzyme was shown to possess at least two binding sites for Mg^{2+} with low and high affinities. The effects of Mg^{2+} binding on the enzymatic activity and structural stability of the enzyme molecule were also studied. The results indicated that the binding of Mg^{2+} to the low-affinity site was essential for the catalysis, but was independent of the substrate binding to the enzyme. It was also indicated that the alkaline denaturation of the enzyme was partly prevented by the Mg^{2+} binding, whereas no significant protective effect was observed against the denaturation by urea. The pH dependence of the kinetic parameters for the hydrolysis of micellar HNP and mixed micellar SM with Triton X-100 (1:10), catalyzed by SMase from *B. cereus*, was studied in the presence of a large amount of Mg^{2+} to saturate both the low- and high-affinity sites. The pH dependence curves of the logarithm of $1/K_m$ for these two kinds of substrates were similar in shape to each other, and showed a single transition. On the other hand, the shapes of the pH dependence curves of the logarithm of k_{cat} for these two kinds of substrates were different from each other. The pH dependence curve for micellar HNP showed three transitions and, counting from the acidic end of the pH region, the first and third transitions having tangent lines with slopes of +1 and −1, respectively. On the other hand, the curve for mixed micellar SM with Triton X-100 showed one large transition with a slope of +1 (the first transition) and a very small transition (the third transition). On the basis of the present results and the three-dimensional structure of bovine pancreatic DNase I, which has a primary structure similar to that of *B. cereus* SMase, we proposed a catalytic mechanism for *B. cereus* SMase based on general-base catalysis.

Key words: catalytic mechanism, denaturation, enzyme kinetics, Mg^{2+} binding, sphingomyelinase.

Sphingomyelinases (SMases, EC 3.1.4.12, sphingomyelin cholinephosphohydrolase) catalyze the hydrolysis of sphingomyelin (SM) to yield ceramide and phosphorylcholine (*1*). Ceramide formed through the activation of SMase may function as a second messenger in mediating cell growth, differentiation, stress responses, and apoptosis (*2*). In mammalian cells, five types of SMases have been described, *i.e.* acidic, acidic Zn^{2+}-dependent, neutral Mg^{2+}-dependent, neutral Mg^{2+}-independent, and alkaline SMases. Two of these types of SMases, the acidic and neutral Mg^{2+}-dependent SMases, may regulate the intracellular levels of ceramide and subsequent ceramide-mediated responses (*3*). Among these five types of SMases, an acidic SMase has been cloned (*4*). Recently, the cloning of a neutral Mg^{2+}-dependent SMase was also reported (*5*).

Bacterial SMases have been found to be kinds of exotoxins from pathogenic bacteria, and have been established to be hemolysins (*1*). The gene of *Bacillus cereus* SMase was cloned and its amino acid sequence was deduced from the nucleotide sequence of the gene (*6*). The mature form of the enzyme is composed of 306 amino acid residues, having a molecular weight of 34 kDa. In the presence of Ca^{2+} or Mn^{2+}, the enzyme is able to be adsorbed specifically to the erythrocyte membrane, while Mg^{2+} extremely enhances the hemolytic activity together with the breakdown of SM (*1*). Although *B. cereus* SMase is different in size from known mammalian SMases, it has been considered to be a useful tool for tissue culture experiments in order to induce elevation of the cellular ceramide level in an attempt to mimic the biological effect of activation of cellular SMases

[1] A part of this work was supported by Grants-in-Aid for the Encouragement of Young Scientists to S.F. and one for Scientific Research to K.I. from the Ministry of Education, Science, Sports and Culture of Japan.

[2] To whom correspondence should be addressed. Tel: +81-726-90-1075, Fax: +81-726-90-1005, E-mail: ikeda@oysun01.oups.ac.jp

Abbreviations: HNP, 2-hexadecanoylamino-4-nitrophenylphosphorylcholine; SM, sphingomyelin; SMase, sphingomyelinase.

(*7-10*).

Chemical modifications of *B. cereus* SMase suggested that acidic amino acid residues such as Asp and Glu are involved in the catalytic and adsorptive activities of the enzyme (*11*). Mutational analyses suggested that Asp 126 and Asp 156 are involved in the substrate recognition, and that Asp 295, His 151, and His 296 are essential for the hydrolytic activity (*12, 13*). Although its three-dimensional structure has not been determined yet, Matsuo *et al.* predicted the three-dimensional structure of *B. cereus* SMase using a protein fold recognition method, which suggested that SMase adopts a structure similar to that of bovine pancreatic DNase I (*14*). According to this predicted structure, several amino acid residues involved in catalysis and specific recognition of the substrate were proposed. This proposal was in good agreement with the results of mutational analysis.

Recently, the cloning of neutral Mg^{2+}-dependent SMases from mouse and man was studied (*5*). The results suggested that the sequences of these proteins were totally conserved with the residues important for the Mg^{2+} binding and for the catalysis of a large family of Mg^{2+}-dependent phosphodiesterases as well as bovine DNase I and *B. cereus* SMase.

In the present study, we investigated the effects of Mg^{2+} binding on the enzyme activity and structural stability, and also the pH dependence of the kinetic parameters for the hydrolysis of micellar 2-hexadecanoylamino-4-nitrophenylphosphorylcholine (HNP) and mixed micellar SM with Triton X-100. We will discuss the participation of ionizable groups in the substrate binding and catalysis, and the catalytic mechanism of SMase.

MATERIALS AND METHODS

Materials—Sphingomyelin (SM) from bovine brain, 2-(*N*-hexadecanoylamino)-4-nitrophenylphosphocholine (HNP) and Triton X-100 were obtained from Sigma. Extra-pure $MgCl_2 \cdot 6H_2O$ and NaCl were obtained from Wako Pure Chemicals and Matsunaga Chemicals, respectively.

Preparation of SMase—SMase from *B. cereus* was prepared by a method similar to that of Tomita *et al.* (*15*) or obtained from Higeta Shooyu. The homogeneity of the prepared and purchased enzymes was confirmed by SDS-PAGE, amino acid analysis, N-terminal sequencing, and reversed-phase HPLC. The elution patterns on reversed-phase HPLC chromatography of the lysyl endopeptidase-digested peptides derived from *S*-pyridylethylated derivatives of the prepared and purchased SMases were practically the same. We also confirmed that the two enzymes have the same enzymatic activity.

The final preparation of the purified enzyme was applied on a column of Sephadex G-100 in order to remove a small amount of aggregated proteins and to replace the solvent with that of a constant ionic strength of 0.2. The purchased preparation of SMase was dissolved in a 8 M urea solution, and then dialyzed against 0.2 M NaCl and centrifuged. The resulting supernatant was applied on a column of Sephadex G-100.

The enzyme concentration was determined spectrophotometrically based on the molar absorption coefficient of 5.82×10^4 $M^{-1} \cdot cm^{-1}$ at 280 nm, which had been calculated from its Tyr and Trp contents (*6*), and the respective molar absorption coefficients of 1.4×10^3 and 5.5×10^3 $M^{-1} \cdot cm^{-1}$ at 280 nm (*16*). The final enzyme solution was stored at −4°C.

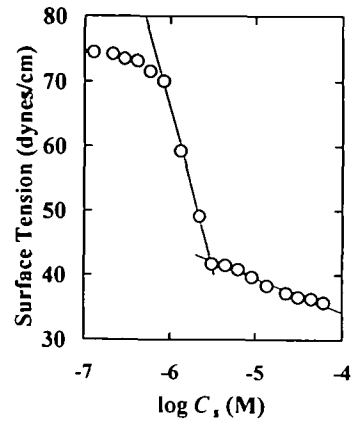

Fig. 1. **Determination of the critical micellar concentration (cmc) of HNP.** The surface tension of a HNP solution in 50 mM Tris-HCl buffer (pH 7.3) containing 4 mM Mg^{2+} at 37°C and ionic strength 0.2 was plotted as a function of the logarithm of the molar concentration of HNP, C_t.

Fluorescence Measurements—The tryptophyl fluorescence spectra were recorded at 25°C and ionic strength 0.2 with a Hitachi model 850 fluorescence spectrophotometer equipped with a spectral corrector. The slit widths for the excitation and emission beams were 2.0 and 10.0 nm, respectively. The excitation wavelength for the measurements was 290 nm. The fluorescence of a reference solution of *N*-acetyl-L-tryptophanamide (Sigma) was measured just before and after measurement of the sample solution, in order to correct for small instrumental fluctuations. The observed fluorescence spectrum was corrected by subtracting the spectrum of a blank solution, which lacked the protein. The final concentration of protein was 1×10^{-7} M.

Determination of the Binding Molar Ratio of Mg^{2+} to SMase—The binding molar ratio of Mg^{2+} to SMase was determined by the equilibrium dialysis method in 20 mM MES buffer at pH 6.0, 25°C, and ionic strength 0.2. One hundred microliters of an enzyme solution containing Mg^{2+} was separated from 100 μl of a Mg^{2+} solution with a dialysis membrane, Spectra/Por (Spectrum. molecular weight cut-off, 12-14 kDa). After reaching equilibration in 24 h at 25°C, the Mg^{2+} concentration in both solutions was determined with an atomic absorption/flame emission spectrophotometer AA-670 (Shimadzu) at 286 nm, which had been calibrated with a standard solution of Mg^{2+} (Wako Pure Chemicals).

Circular Dichroism (CD) Measurements—CD spectra were recorded in the far-ultraviolet region at 37°C and ionic strength 0.2 with a Jasco model J-500A spectropolarimeter, which had been calibrated with a standard solution of ammonium *d*-camphorsulfonate (Katayama Chemicals). A cell of 0.1 or 0.2 cm pathlength was used for the measurements. The protein concentrations were 0.04-0.05 mg/ml. The mean residue ellipticity, $[\theta]$, was obtained with the equation: $[\theta] = (100 \times \theta)/(l \times c)$, where θ is the observed ellipticity in degrees, l the pathlength of the cell in centimeters, and c the residue molar concentration of

protein. An average residue weight of 112 was used to calculate the residue molar concentration.

Determination of the Critical Micellar Concentration (cmc) of HNP—The surface tension of a HNP solution in 50 mM Tris-HCl buffer (pH 7.3) containing 4 mM Mg^{2+} was measured at 37°C and ionic strength 0.2 with a Du Noüy's tensionmeter. Figure 1 shows the surface tension as a function of the logarithm of the molar concentration of HNP, C_s. The cmc value was determined to be 3.1 μM from the break in the titration curve. All the experiments below were therefore performed with a concentration of HNP above the cmc (where HNPs are in micellar states).

SMase Activity Measurements—The hydrolysis of HNP catalyzed by SMase was measured according to the method of Gal *et al.* (*17*) at 37°C and ionic strength 0.2. Enzymatic hydrolysis was initiated by the addition of 5–10 μl of the enzyme stock solution to 100 μl of the substrate solution containing a given concentration of Mg^{2+}. After the reaction mixture had been incubated for appropriate times, 3 ml of 0.1 M glycine-NaOH buffer (pH 10.5) was added so as to quench the enzyme reaction. The absorbance at 410 nm of the solution was measured and the enzyme activity was calculated using the molar absorption coefficient of 2′-hydroxy-5′-nitrohexadecananilide, $\varepsilon = 1.49 \times 10^4\ M^{-1} \cdot cm^{-1}$, at 410 nm.

The hydrolysis of mixed micellar SM with Triton X-100 catalyzed by SMase was followed at 25°C and ionic strength 0.2 by the pH-stat assay method using a system consisting of a Radiometer PHM 82 standard pH meter, a TTT 80 titrator, and an ABU 80 autoburette. The substrate solutions containing various concentrations of $MgCl_2$ were transferred to separate cells, and then the pH of the solutions was adjusted to desired values by the addition of small volumes of a 10 mM NaOH solution. To these solutions, 10–20 μl of the enzyme stock solution was added and then the released phosphorylcholine was titrated with 10 mM NaOH under a nitrogen stream so as to keep the pH at the initial value. At pH values below 7, the observed titration volumes are the apparent values, since the phosphate moiety of the released phosphorylcholine molecule would not completely dissociate in this pH range. The observed titration volumes were therefore corrected by use of the degree of dissociation, α, of phosphorylcholine at a given pH value: $\alpha = 1/(1+10^{pK-pH})$, where $pK(=5.72)$ is the dissociation constant (*18*).

Buffer Solutions—The assay solutions, which were used for the experiments for the fluorescence spectra, CD spectra, and enzyme activity toward micellar HNP, contained buffer components at final concentrations of 45, 20, and 45 mM, respectively. The buffer components used were acetic acid, 2-morpholinoethanesulfonate (MES), 2-[4-(2-hydroxyethyl)-2-piperazinyl]ethanesulfonate (HEPES), *N*-tris-(hydroxymethyl)methyl-3-aminopropanesulfonate (TAPS), and *N*-cyclohexyl-2-hydroxy-3-aminopropanesulfonate (CAPSO), all of which were from Nacalai Tesque (Kyoto). The buffer solutions were prepared with NaCl added to give 0.2 ionic strength. The final pH values of the protein solutions were read at 25 or 37°C with a Radiometer PHM 82 pH meter.

RESULTS

Binding of Mg^{2+} to SMase—The inset in Fig. 2 compares the fluorescence spectra, with excitation at 290 nm, of *B. cereus* SMase in the presence and absence of Mg^{2+} at 25°C, pH 6.0, and ionic strength 0.2. The fluorescence maximum at 340 nm decreased slightly in intensity as Mg^{2+} bound to the enzyme.

Figure 2 shows the decrease in the fluorescence intensity at 340 nm, $|\Delta F|$, and the initial velocity of the hydrolysis of micellar HNP in the presence of a saturating amount of it, v, plotted as a function of the logarithm of the molar concentration of Mg^{2+}, C_M. Since the change in the fluorescence intensity on the addition of Mg^{2+} was very small (see inset in Fig. 2), the measurement was carefully performed. In the Mg^{2+}-dependence curve of $|\Delta F|$, two distinct transitions were observed, suggesting the existence of at least two binding sites for Mg^{2+} with high and low affinities. If each of these binding sites can bind one molecule of Mg^{2+}, the interaction scheme can be expressed as

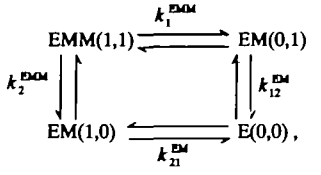

where E and M represent the enzyme and Mg^{2+}, respectively. EM and EMM represent the enzyme complex with one and two molecules of Mg^{2+}, respectively. The first and second numerals in parentheses indicate the states of the two distinct binding sites for Mg^{2+}; 1 and 0 indicate their respective bound and unbound states. k_1^{EMM} and k_2^{EMM} are the microscopic dissociation constants of Mg^{2+} from EMM(1,1) to EM(0,1) and EM(1,0), respectively, and k_{12}^{EM} and k_{21}^{EM} are those from EM(0,1) and EM(1,0) to E(0,0), respectively.

The $|\Delta F|$ value observed at a given molar concentration

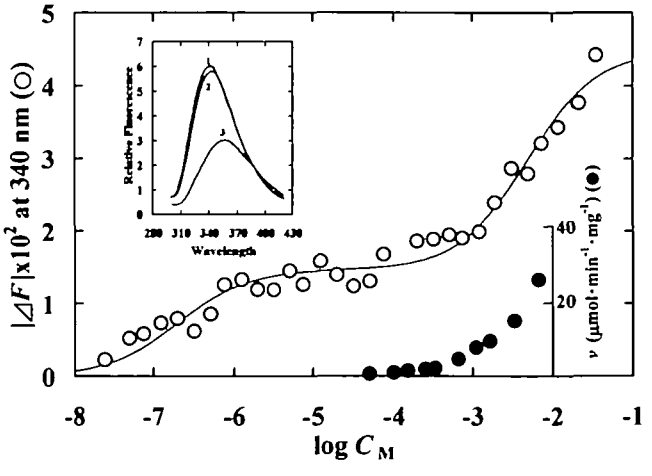

Fig. 2. **Fluorescence change at 340 nm, with excitation at 290 nm, of *B. cereus* SMase, $|\Delta F|$ (○), on the addition of Mg^{2+} at 25°C, pH 6.0, and ionic strength 0.2, plotted as a function of the logarithm of the total concentration of Mg^{2+}, C_M.** This figure also shows the change in the initial velocity of the hydrolysis of HNP, v (●), catalyzed by SMase in the presence of saturating amounts of the substrate at 37°C, pH 6.0, and ionic strength 0.2. The inset shows the fluorescence spectra of SMase, with excitation at 290 nm and measured at 25°C, pH 6.0, and ionic strength 0.2. 1, apoenzyme in the presence of 0.1 mM EDTA; 2, the Mg^{2+}-complex in the presence of 47 mM Mg^{2+}; 3, *N*-acetyl-L-tryptophanamide at the same molar concentration as the tryptophan in the enzyme molecule.

of Mg^{2+}, C_M, can be expressed as

$$|\Delta F| = \frac{A \cdot C_M + B \cdot C_M^2}{1 + \frac{C_M}{K^{EM}} + \frac{C_M^2}{K^{EMM} \cdot K^{EM}}}, \quad (1)$$

where K^{EMM} and K^{EM} are the macroscopic dissociation constants of Mg^{2+} from EMM to EM[=EM(1,0)+EM(0, 1)], and from EM to E, respectively. A and B are the constants expressed as

$$A = \frac{|\Delta F_{EM(1,0)}|}{k_{21}^{EM}} + \frac{|\Delta F_{EM(0,1)}|}{k_{12}^{EM}} \quad (2)$$

and

$$B = \frac{|\Delta F_{EMM(1,1)}|}{K^{EMM} \cdot K^{EM}}, \quad (3)$$

where $|\Delta F_{EM(1,0)}|$, $|\Delta F_{EM(0,1)}|$, and $|\Delta F_{EMM(1,1)}|$ are the limiting values of $|\Delta F|$ for the microscopic complex forms of EM(1, 0), EM(0,1), and EMM(1,1), respectively. The solid curve shown in Fig. 2 is the most probable theoretical one, drawn according to Eq. 1 by use of the parameters, $1/K^{EMM} = 2.1 \times 10^2\ M^{-1}$, $1/K^{EM} = 5.0 \times 10^6\ M^{-1}$, $A = 7.3 \times 10^4\ M^{-1}$, and $B = 4.7 \times 10^7\ M^{-2}$.

Since the dissociation constant of Mg^{2+} for the high-affinity site was of the order of less than μM, its value could not be estimated accurately. But, the existence of this high-affinity site was confirmed by the equilibrium dialysis method. After reaching equilibration in 24 h, the concentrations of Mg^{2+} in the solutions in the compartment containing 22.3 μM enzyme and in that lacking the enzyme were determined to be 202 and 181 μM, respectively, from which the concentration of Mg^{2+} bound to the enzyme was calculated to be 21 μM, indicating that about one Mg^{2+} molecule is bound to one enzyme molecule at an equilibrium concentration of 181 μM Mg^{2+} ($\log C_M = -3.74$). This result suggests that one Mg^{2+} molecule can occupy this high-affinity binding site below this Mg^{2+} concentration. The number of Mg^{2+} molecules bound to the low-affinity site could not be determined by this method, since SMase can not be dissolved at the concentration of more than 50 μM required for this purpose.

Effect of Mg^{2+} on the Denaturation of SMase by Urea—Figure 3A shows the tryptophyl fluorescence spectra of *B. cereus* SMase in the presence of 1.0 mM EDTA at several concentrations of urea at 25°C, pH 6.0, and ionic strength 0.2, after the solutions had been stood for 24 h at room temperature. The fluorescence intensity decreased and the fluorescence maxima red-shifted as the concentration of urea increased. The spectrum in the presence of 7.5 M urea was similar to that of *N*-acetyl-L-tryptophanamide at the same molar concentration as the tryptophyl residues of the SMase molecule (*B. cereus* SMase contains 6 Trp residues), indicating complete denaturation of this protein.

Figure 3B shows the effect of Mg^{2+} on the urea denaturation of *B. cereus* SMase studied by using the changes in the tryptophyl fluorescence intensity. SMase was completely denaturated with 6 M urea. The denaturation curves of SMase in the presence of 0.7 and 53 mM Mg^{2+} were shown to be essentially the same as that in the absence of Mg^{2+}.

Stability of SMase as to pH Change—The far-ultraviolet CD spectrum of *B. cereus* SMase, in the presence of 1.0 mM EDTA at pH 6.83, 37°C and ionic strength 0.2, is shown in the inset in Fig. 4. Figure 4 also shows the pH dependence of the negative ellipticity at 222 nm of this enzyme.

Above pH 9.0 and below pH 5.0, the negative ellipticity decreased with time, indicating protein denaturation.

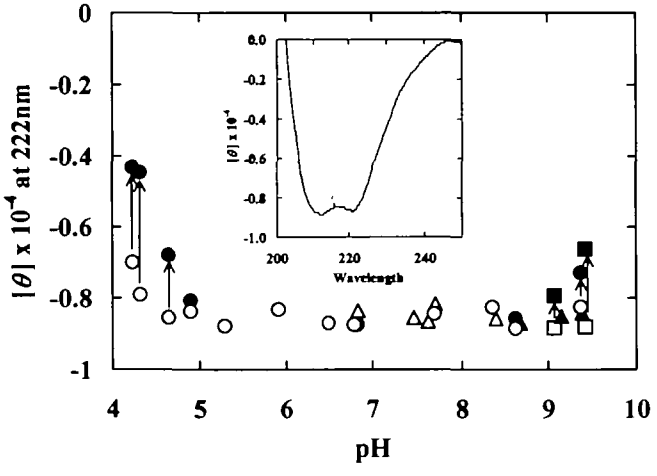

Fig. 4. **pH dependence of the negative ellipticity at 222 nm of *B. cereus* SMase in the presence of 1.0 mM EDTA (circles), 1.1 μM Mg^{2+} (squares), and 22 mM Mg^{2+} (triangles) at 37°C and ionic strength 0.2.** The filled symbols indicate the data after 30 min. The inset shows the CD spectrum in the presence of 1.0 mM EDTA at 37°C, pH 6.83, and ionic strength 0.2.

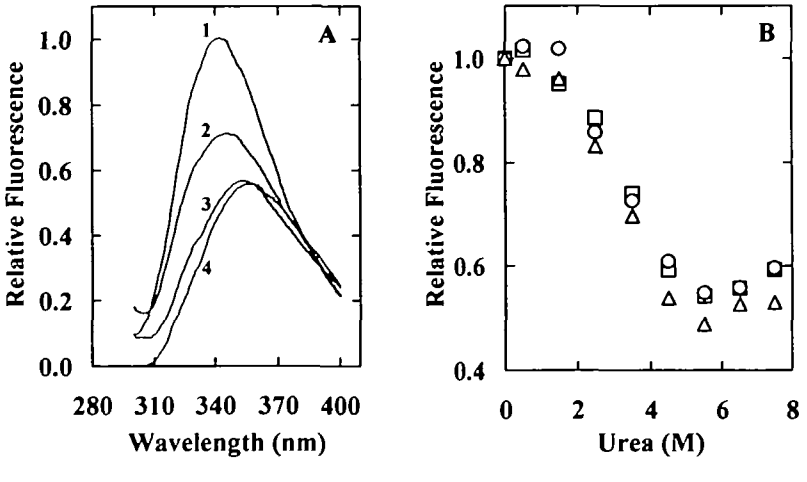

Fig. 3. **Effect of Mg^{2+} on the denaturation of *B. cereus* SMase by urea.** The solutions were allowed to stand for 24 h at room temperature. A: Fluorescence spectra of SMase, with excitation at 290 nm and measured at 25°C, pH 6.0, and ionic strength 0.2 in the presence of 1.0 mM EDTA. 1, 0 M urea; 2, 3.5 M urea; 3, 7.5 M urea; 4, *N*-acetyl-L-tryptophanamide at the same molar concentration as the tryptophan in the enzyme molecule. B: Urea denaturation curves for SMase in the presence of 0 mM (○), 0.7 mM (△), and 53 mM (□) Mg^{2+} at 25°C, pH 6.0, and ionic strength 0.2. The fluorescence intensity, with excitation at 290 nm, was measured at 340 nm.

Denaturation of this protein above pH 9.0 was prevented in the presence of 22.2 mM Mg^{2+}, but not in the presence of 1.1 μM Mg^{2+}. In the acid pH range, the effect of Mg^{2+} on the structural stability of SMase as to pH change could not be studied, since the binding constants of Mg^{2+} were too small below pH 5.0 (described below).

All the experiments below were therefore performed in the pH range of 5.0 to 9.0, in which this enzyme is structurally stable.

Effect of Mg^{2+} on the Enzymatic Hydrolysis of HNP and SM—Figure 5A shows Lineweaver-Burk plots for the hydrolysis of micellar HNP by *B. cereus* SMase at 37°C, pH 6.0, and ionic strength 0.2 in the presence of various concentrations of Mg^{2+}. Figure 6A shows plots similar to those in Fig. 5A for mixed micellar SM with Triton X-100 (1:10) used as a substrate at 25°C. The Mg^{2+} concentrations used were enough to saturate the high-affinity binding site for Mg^{2+} (see Fig. 2). The apparent maximum velocity, V_{max}^{app}, and apparent Michaelis constant, K_m^{app}, values were determined from the respective hyperbolic curves of velocity data by means of nonlinear regression analysis.

For both substrates, V_{max}^{app} increased with an increase in the concentration of Mg^{2+} whereas K_m^{app} remained unchanged.

A putative interaction scheme can be expressed as

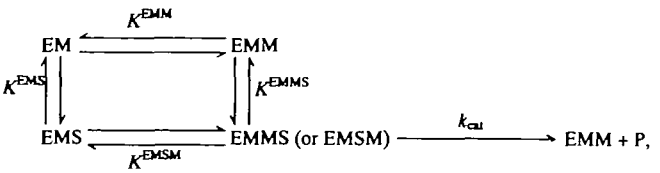

where E, M, S, and P represent the enzyme, Mg^{2+}, substrate, and product, respectively. EM and EMS represent the enzyme-Mg^{2+} complex and enzyme-Mg^{2+}-substrate complex, respectively, where the high-affinity binding site for Mg^{2+} is occupied. EMM and EMMS represent the respective Mg^{2+} complexes, where both the high- and low-affinity binding sites for Mg^{2+} are saturated. K^{EMM} and K^{EMSM} are the dissociation constants of Mg^{2+} as to the low-affinity site of the enzyme-Mg^{2+} complex (EMM) and the enzyme-substrate-Mg^{2+} complex (EMSM), respectively. K^{EMS} and K^{EMMS} are the dissociation constants of substrate as to the EMS and EMMS complexes, respectively. Among these dissociation constants, a linked relationship, $K^{EMM} \cdot K^{EMMS} = K^{EMS} \cdot K^{EMSM}$, exists. The kinetic parameters, K_m^{app}/V_{max}^{app} and $1/V_{max}^{app}$, which were obtained at a given molar concentration of Mg^{2+}, C_M, can thus be expressed with the equations:

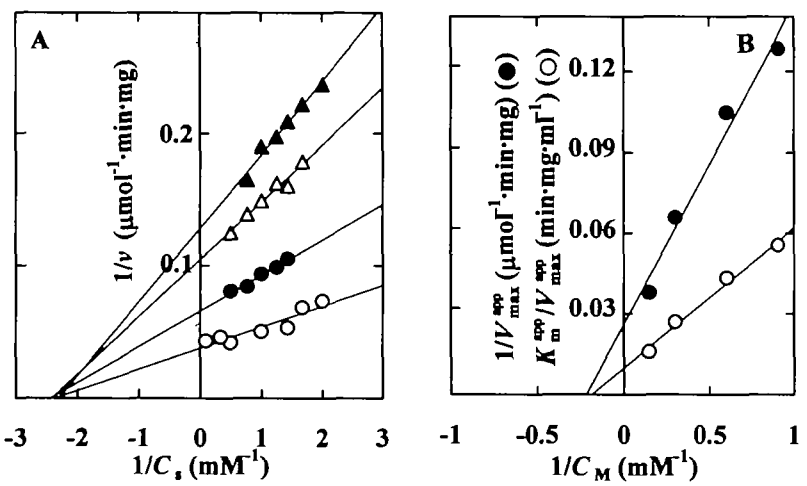

Fig. 5. **Effect of Mg^{2+} on the kinetics of the hydrolysis of micellar HNP, catalyzed by *B. cereus* SMase at 37°C, pH 6.0, and ionic strength 0.2.** A: Lineweaver-Burk plots of the kinetic data in the presence of 6.67 mM (○), 3.33 mM (●), 1.67 mM (△), and 1.11 mM (▲) Mg^{2+}. B: The reciprocal of the apparent maximum velocity, $1/V_{max}^{app}$ (●), and the apparent parameter, K_m^{app}/V_{max}^{app} (○), were each plotted as a function of the reciprocal of Mg^{2+} concentration, $1/C_M$, according to Eqs. 4 and 5, respectively.

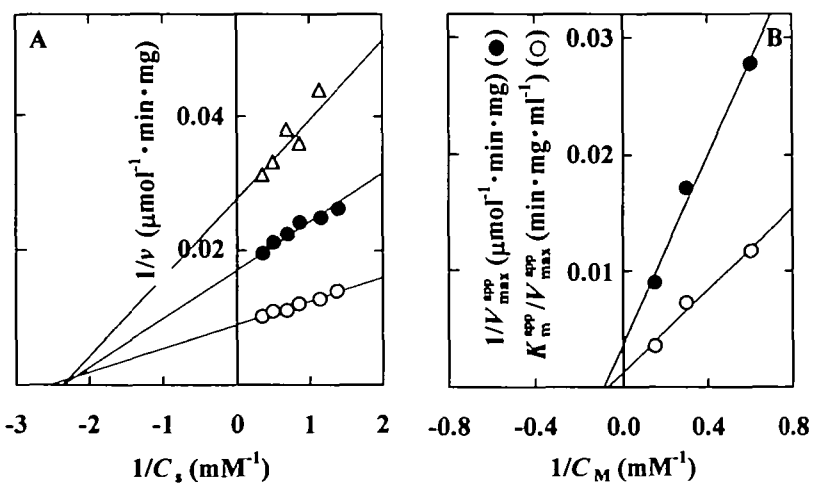

Fig. 6. **Effect of Mg^{2+} on the kinetics of the hydrolysis of mixed micellar SM with Triton X-100 (1:10), catalyzed by *B. cereus* SMase at 25°C, pH 6.0, and ionic strength 0.2.** A: Lineweaver-Burk plots of the kinetic data in the presence of 6.67 mM (○), 3.33 mM (●), and 1.67 mM (△). B: The reciprocal of the apparent maximum velocity, $1/V_{max}^{app}$ (●), and the apparent parameter, K_m^{app}/V_{max}^{app} (○), were each plotted as a function of $1/C_M$ according to Eqs. 4 and 5, respectively.

$$\frac{K_m^{app}}{V_{max}^{app}} = \frac{K_m \cdot K^{EMM}}{V_{max}} \cdot \frac{1}{C_M} + \frac{K_m}{V_{max}} \quad (4)$$

and

$$\frac{1}{V_{max}^{app}} = \frac{K^{EMSM}}{V_{max}} \cdot \frac{1}{C_M} + \frac{1}{V_{max}}, \quad (5)$$

where K_m and V_{max} are the Michaelis constant and maximum velocity when the enzyme is saturated with Mg^{2+} at both the high- and low-affinity binding sites. The parameter, K_m, may correspond to K^{EMMS}, which appears in the interaction scheme, described above. Figures 5B and 6B show the K_m^{app}/V_{max}^{app} and $1/V_{max}^{app}$ values for the two kinds of substrates plotted as a function of $1/C_M$ according to Eqs. 4 and 5, respectively.

From the plots in Fig. 5B, the values of $1/K^{EMM}$ and $1/K^{EMSM}$ were determined to be $1.9 \pm 0.5 \times 10^2\ M^{-1}$ and $2.2 \pm 0.7 \times 10^2\ M^{-1}$, respectively. From the plots in Fig. 6B, as corresponding values, similar values were obtained: $0.73 \pm 0.56 \times 10^2\ M^{-1}$ and $0.90 \pm 0.47 \times 10^2\ M^{-1}$, respectively, although a different substrate, SM, was used. All these values approximately agreed with those determined on fluorescence measurement (Fig. 2).

pH Dependence of the Binding Constants of Mg^{2+} as to the Low-Affinity Site—As the concentration of Mg^{2+} increased, the fluorescence intensity of *B. cereus* SMase slightly decreased (see inset in Fig. 2). By using this decrease in the fluorescence intensity at 340 nm, $|\Delta F|$, the binding constant of Mg^{2+} as to the low-affinity site, $1/K^{EMM}$, could be determined according to Eq. 1. To obtain this kind of binding constant efficiently and precisely at various pH values, the experiments were performed solely in the range of Mg^{2+} concentrations in which Mg^{2+} bound to the low-affinity site, and the data were analyzed according to the equation:

$$|\Delta F|/C_M = -\frac{1}{K^{EMM}}(|\Delta F| - |\Delta F_{EMM}|), \quad (6)$$

where $|\Delta F_{EMM}|$ is the limiting value of $|\Delta F|$ for the complete Mg^{2+} complex with both the binding sites being saturated with Mg^{2+}. C_M is the molar concentration of free Mg^{2+}, which could be replaced by the total molar concentration of Mg^{2+}, since the molar concentration of protein was far lower than the total molar concentration of Mg^{2+}.

Figure 7A shows the data at three pH values, plotted according to Eq. 6. The $1/K^{EMM}$ and $|\Delta F_{EMM}|$ values were determined from the negative slopes of the straight lines and from the intercepts on the abscissas, respectively.

Figure 7, B and C, shows double reciprocal plots of the initial velocity and Mg^{2+} concentration for the hydrolysis of micellar HNP catalyzed by SMase at 37°C and ionic strength 0.2. Since the experiment was performed at substrate concentrations which can practically saturate the enzyme, the initial velocity could be replaced by V_{max}^{app} in Eq. 5. The binding constants of Mg^{2+} as to the low-affinity binding site of the enzyme-Mg^{2+}-substrate complex, $1/K^{EMSM}$, and the V_{max} values were determined from the intercepts on the abscissa and ordinate, respectively.

Figure 8 shows the pH dependence of the logarithm of the binding constant of Mg^{2+} as to the low-affinity binding site of SMase determined from Fig. 7. This figure also includes

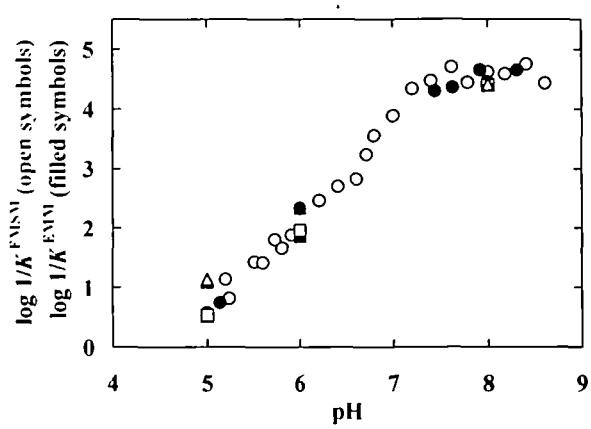

Fig. 8. **pH dependence of the logarithm of the binding constant of Mg^{2+} as to the low-affinity site of *B. cereus* SMase.** The $1/K^{EMM}$ (●) and $1/K^{EMSM}$ (○) data were obtained from the Scatchard plots in Fig. 7A, and the double reciprocal plots in Fig. 7, B and C, respectively. The data indicated by triangles and squares were obtained from the double reciprocal plots in Figs. 5B and 6B, respectively, and the filled and open symbols represent $1/K^{EMM}$ and $1/K^{EMSM}$, respectively. The $1/K^{EMM}$ (◆) value was obtained from the data in Fig. 2.

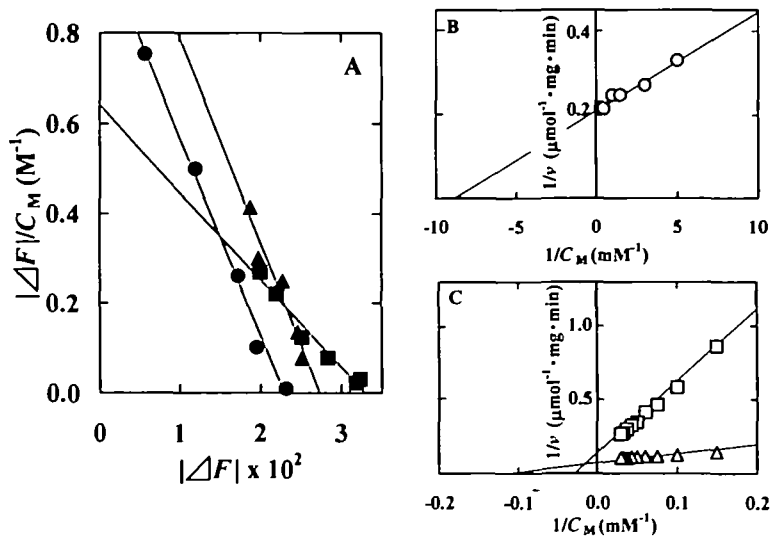

Fig. 7. **Determination of the binding constant of Mg^{2+} as to the low-affinity site of *B. cereus* SMase.** A: Scatchard plots of the changes in the fluorescence intensities at 340 nm, $|\Delta F|$, with the molar concentration of Mg^{2+}, C_M, at 25°C and ionic strength 0.2. ●, pH 8.31; ▲, pH 7.92; ■, pH 7.44. B and C: Double reciprocal plots of the initial velocity, v, and Mg^{2+} concentration, C_M, for the hydrolysis of micellar HNP catalyzed by SMase in the presence of saturating amounts of the substrate at 37°C and ionic strength 0.2. ○, pH 8.0; △, pH 6.0; □, pH 5.0.

the binding constants determined in the experiments at pH 5.0, 6.0, and 8.0 shown in Figs. 2, 5, and 6. In the pH range studied, the binding of Mg^{2+} to the low-affinity binding site was confirmed to be independent of the substrate binding to the enzyme, since the $1/K^{EMM}$ and $1/K^{EMSM}$ values were very similar to each other at individual pH values.

pH Dependence of the Kinetic Parameters for the Hydrolysis of Micellar HNP and Mixed Micellar SM with Triton X-100—Figure 9 shows the pH dependence of the logarithm of $1/K_m$ for the enzymatic hydrolysis of micellar HNP, catalyzed by *B. cereus* SMase at 37°C and ionic strength 0.2 in the presence of Mg^{2+}, which can practically saturate both the low- and high-affinity binding sites. This figure also shows similar data for mixed micellar SM with Triton X-100 (1:10) at 25°C. The K_m values could be directly replaced by the K_m^{app} values, which had been determined from the respective hyperbolic curves of velocity *vs.* substrate concentration by nonlinear regression analysis, since the substrate binding was independent of the Mg^{2+} binding, as described above (Figs. 5 and 6). The pH dependence curves for the two substrates showed a single transition between pH 6 and 7, suggesting the participation of one ionizable group.

An interaction scheme for analyzing this pH dependence of substrate binding might be expressed as

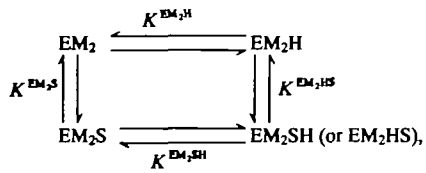

where EM_2 and EM_2H represent the microscopic forms of the deprotonated and protonated enzyme-Mg^{2+} complexes having Mg^{2+}-suturated high- and low-affinity binding sites, respectively. EM_2S and EM_2SH represent the microscopic forms of the deprotonated and protonated enzyme-Mg^{2+}-substrate complexes, respectively. K^{EM_2S} and K^{EM_2HS} are the dissociation constants of the substrate as to EM_2S and its protonated form (EM_2HS), respectively. K^{EM_2H} and K^{EM_2SH} are the dissociation constants of the protons as to EM_2H and EM_2SH, respectively. The logarithm of $1/K_m$, obtained at a given pH value may therefore be expressed as

$$\log\frac{1}{K_m}=\log\frac{\frac{[H^+]}{K^{EM_2SH}}+1}{\frac{[H^+]}{K^{EM_2H}}+1}+\log\frac{1}{k_m}, \quad (7)$$

where $1/k_m$ is the limiting value of $1/K_m$ when the ionizable group in question is completely deprotonated ($=1/K^{EM_2S}$).

The solid and broken curves in Fig. 9 are the most probable theoretical ones, drawn according to Eq. 7 using the parameters of $pK^{EM_2SH}=6.05$, $pK^{EM_2H}=6.81$, and $1/k_m=1.00\times10^4\ M^{-1}$ for micellar HNP, and $pK^{EM_2SH}=6.06$, $pK^{EM_2H}=6.81$, and $1/k_m=9.71\times10^3\ M^{-1}$ for mixed micellar SM with Triton X-100, respectively.

Figure 10 shows the pH dependence of the logarithm of k_{cat} for the enzymatic hydrolysis of micellar HNP catalyzed by *B. cereus* SMase at 37°C and ionic strength 0.2 in the presence of a practically saturating amount of Mg^{2+}. This figure also shows similar data for mixed micellar SM with Triton X-100 (1:10) at 25°C. The k_{cat}^{app} values, which had been determined from the respective hyperbolic curves of velocity *vs.* substrate concentration by nonlinear regression analysis, were corrected to the values, k_{cat}, for the complete Mg^{2+} complexes by using the $K^{EMM}(=K^{EMSM})$ values, which had been obtained from Fig. 8.

The pH dependence curve of k_{cat} for the micellar HNP showed three transitions, below pH 6, between pH 6.5 and 7, and above pH 7.5, respectively, suggesting the participation of three ionizable groups. The first large transition below pH 6, which was also observed for the other kind of substrate (mixed micellar SM with Triton X-100), has a tangent line with a slope of +1, and the ionizable group participating in this transition seems to be crucially important for catalysis.

Regarding the ionization states of the three groups in question, there are eight microscopic forms of the enzyme-Mg^{2+}-substrate complex: $EM_2SH_3(1,1,1)$, $EM_2SH_2(1,1,0)$,

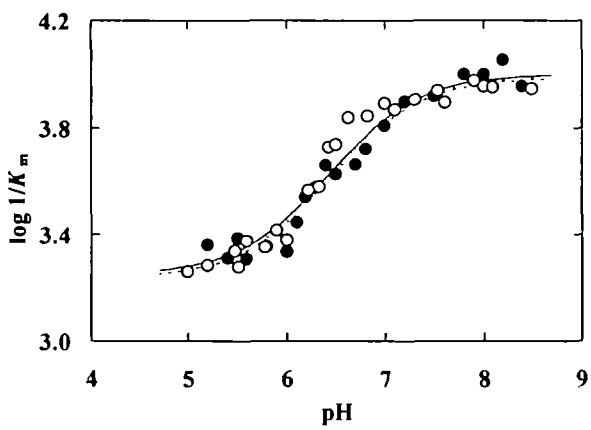

Fig. 9. **pH dependence of the logarithm of $1/K_m$ for the hydrolysis of micellar HNP (○) and mixed micellar SM with Triton X-100 (1:10) (●), catalyzed by *B. cereus* SMase at a Mg^{2+} concentration enough to saturate both the high- and low affinity binding sites at ionic strength 0.2.** The solid and broken curves for HNP and SM, respectively, are the theoretical ones constructed according to Eq. 7 using the parameters given in the text.

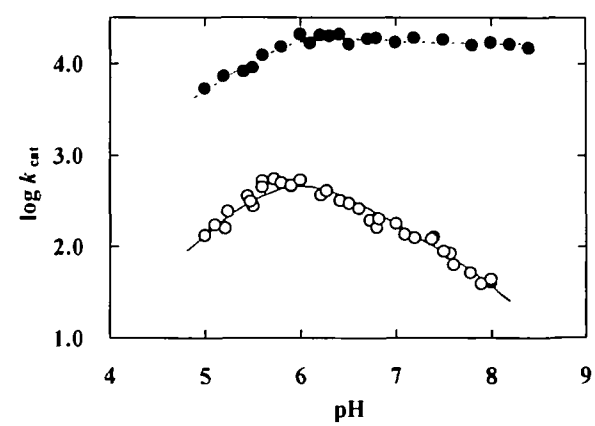

Fig. 10. **pH dependence of the logarithm of $1/k_{cat}$ for the hydrolysis of micellar HNP (○) and mixed micellar SM with Triton X-100 (1:10) (●), catalyzed by *B. cereus* SMase at a Mg^{2+} concentration enough to saturate both the high- and low-affinity binding sites at ionic strength 0.2.** The solid and broken curves for HNP and SM, respectively, are the theoretical ones constructed according to Eq. 8 using the parameters given in the text.

$EM_2SH_2(1,0,1)$, $EM_2SH_2(0,1,1)$, $EM_2SH(1,0,0)$, $EM_2SH(0,1,0)$, $EM_2SH(0,0,1)$, and $EM_2S(0,0,0)$, where the first, second, and third numerals in parentheses represent the ionization states of the three ionizable groups participating in the transitions below pH 6, between pH 6.5 and 7, and above pH 7.5, respectively; 1 and 0 indicate their respective protonated and deprotonated states. Among these eight molecular complexes, only four species having the deprotonated form of the first ionizable group, $EM_2SH_2(0,1,1)$, $EM_2SH(0,1,0)$, $EM_2SH(0,0,1)$, and $EM_2S(0,0,0)$, were assumed to produce the product, with rate constants of $k_{cat,1}$, $k_{cat,2}$, $k_{cat,3}$, and $k_{cat,4}$, respectively, since the protonated state of this group seemed to be inactive as to catalysis toward both the substrates. Figure 11 shows the reaction scheme proposed.

The logarithm of k_{cat} observed at a given pH value may therefore be expressed as

$$\log k_{cat} = \log \frac{A\cdot[H^+]^2+B\cdot[H^+]+C}{\frac{[H^+]^3}{K^{EM_2SH_2}\cdot K^{EM_2SH_2}\cdot K^{EM_2SH_1}}+\frac{[H^+]^2}{K^{EM_2SH_2}\cdot K^{EM_2SH_1}}+\frac{[H^+]}{K^{EM_2SH_1}}+1}, \quad (8)$$

where $K^{EM_2SH_2}$, $K^{EM_2SH_2}$, and $K^{EM_2SH_1}$ are the macroscopic dissociation constants of the protons as to the three ionizable groups in question of the enzyme-Mg^{2+}-substrate complex. A, B, and C are the respective constants expressed as

$$A = \frac{k_{cat,1}}{k_{12}^{EM_2SH_2}\cdot k_{123}^{EM_2SH}}, \quad (9)$$

$$B = \frac{k_{cat,2}}{k_{132}^{EM_2SH}} + \frac{k_{cat,3}}{k_{123}^{EM_2SH}}, \quad (10)$$

and

$$C = k_{cat,4}, \quad (11)$$

where $k_{12}^{EM_2SH_2}$ is the microscopic dissociation constant of the protons as to $EM_2SH_2(0,1,1)$ to $EM_2SH(0,0,1)$, and $k_{132}^{EM_2SH}$ and $k_{123}^{EM_2SH}$ are those as to $EM_2SH(0,1,0)$ and $EM_2SH(0,0,1)$ to $EM_2S(0,0,0)$, respectively.

In the case of micellar HNP used as a substrate, the transitions above pH 7.5 involving in the third ionizable group seemed to have a tangent line with a slope of -1. Therefore, only two microscopic forms having deprotonated and protonated forms of the respective first and third ionizable groups, $EM_2SH_2(0,1,1)$ and $EM_2SH(0,0,1)$, were assumed to produce the product, and $k_{cat,2}$ and $k_{cat,4}$ in Eqs. 10 and 11 could be neglected. By assuming that the pK value of the second ionizable group is the same as the pK value of the enzyme-Mg^{2+}-substrate complex, $K^{EM_2SH_2} = 6.05$, which had been determined from the pH dependence data for $1/K_m$, parameters $pK^{EM_2SH_2}$, $pK^{EM_2SH_1}$, A, and B were determined to be 5.85, 7.60, 4.88×10^{16} $M^{-2}\cdot min^{-1}$, and 4.68×10^{9} $M^{-1}\cdot min^{-1}$, respectively, according to Eq. 8, where B was substituted with $k_{cat,3}/k_{123}^{EM_2SH}$ and C was neglected.

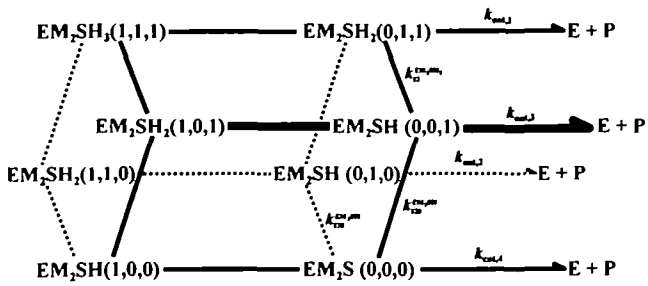

Fig. 11. A scheme for the product formation from four of the eight microscopic forms of the enzyme-Mg^{2+}-substrate complex, in which both the low- and high-affinity Mg^{2+} binding sites are saturated.

In the case of mixed micellar SM with Triton X-100, only one large transition having a tangent line with a slope of +1 was observed below pH 6, *i.e.* no clear large transitions were observed in the alkaline pH region. Nevertheless, we assumed that the three ionizable groups participate in the catalytic activity toward mixed micellar SM with Triton X-100, since the catalytic mechanism should be common regardless of the substrate used. The data were similarly analyzed according to Eq. 8, by assuming that the complex with the deprotonated form of the third group is active in catalysis to form the product. By including in Eq. 8, $K^{EM_2SH_2} = 6.06$, which had been determined from the pH dependence of $1/K_m$, and $K^{EM_2SH_2} = 5.85$ and $K^{EM_2SH_1} = 7.60$, which had been determined from the pH dependence of k_{cat} for the hydrolysis of micellar HNP, parameters A, B, and C were determined to be 1.30×10^{15} $M^{-2}\cdot min^{-1}$, 3.33×10^{10} $M^{-1}\cdot min^{-1}$, and 1.64×10^{4} min^{-1}, respectively.

The solid and broken curves in Fig. 10 are the most probable theoretical ones, and they well fit the pH dependence data for both the substrates.

DISCUSSION

Mg^{2+} Binding of B. cereus SMase—Since the enzyme activity of *B. cereus* SMase requires the binding of Mg^{2+} to the enzyme (*1*), we determined the binding constant of Mg^{2+} on the basis of the changes in the tryptophyl fluorescence intensity. As can be seen from Fig. 2, this enzyme was shown to have at least two binding sites for Mg^{2+} with binding constants of 2.1×10^2 and about 5.0×10^6 M^{-1} at pH 6.0. To confirm the existence of such a high-affinity site for Mg^{2+}, equilibrium dialysis experiments were performed in the presence of about 0.2 mM Mg^{2+}, and the high-affinity site was proved to be practically saturated with one molecule of Mg^{2+}.

In order to clarify the role of the Mg^{2+} binding in the catalytic action of *B. cereus* SMase, enzyme activities were measured in the presence of various concentrations of Mg^{2+}. As can be seen from Fig. 2, the enzymatic activity of SMase paralleled the extent of Mg^{2+} binding to the low-affinity binding site and almost completely disappeared in the presence of Mg^{2+} below 0.1 mM, suggesting that the binding of Mg^{2+} to the low-affinity site is essential for the catalysis. As can be seen from Figs. 5 and 6, the binding of either substrate (HNP or SM) to *B. cereus* SMase is essentially independent of the Mg^{2+} binding to the low-affinity site of the enzyme. The Mg^{2+} binding to the low-affinity site is also independent of the substrate binding (Fig. 8).

The effects of Mg^{2+} on the structural stability of *B. cereus* SMase as to urea and alkaline denaturation were studied. As can be seen from Fig. 3, even in the presence of saturating amounts of Mg^{2+}, the urea denaturation curves were unchanged at pH 6.0. On the other hand, the alkaline denaturation was dependent on the incubation time, and was prevented by the presence of 22.2 mM Mg^{2+}, with

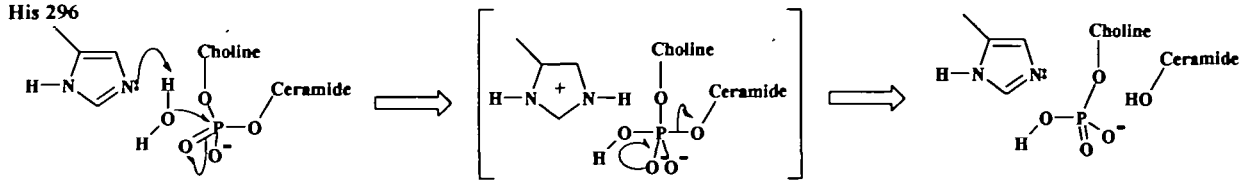

Fig. 12. **The proposed catalytic mechanism of *B. cereus* SMase on the basis of general-base catalysis.**

which both the low- and high-affinity binding sites are saturated with Mg^{2+} (Fig. 4). These results suggest that the Mg^{2+} binding prevents the alkaline denaturation accompanied by the change in the electrostatic interactions, but not the urea denaturation accompanied by the change in the hydrophobic interactions.

Catalytic Function of B. cereus SMase—In the present study, we examined the pH dependence of the logarithms of $1/K_m$ and k_{cat} for the hydrolysis of two kinds of substrates, micellar HNP and mixed micellar SM with Triton X-100, catalyzed by *B. cereus* SMase. As can be seen from Fig. 9, the curves of $1/K_m$ for the two kinds of substrates were very similar in shape to each other and showed a single transition, suggesting the participation of an ionizable group with a pK value of 6.81. The pK values shifted to 6.05 and 6.06 on the binding of HNP and SM, respectively, indicating that the deprotonation of this ionizable group enhances the binding of both types of substrates. This ionizable group was assigned as Asp 126, since a mutant SMase (D126G) whose Asp 126 had been converted to a glycine residue showed no transitions in the pH dependence curve of $1/K_m$ (Fujii *et al.*, to be published).

As can be seen from Fig. 10, the pH dependence curves of k_{cat} for micellar HNP and mixed micellar SM with Triton X-100 were different in shape from each other. The curve for HNP showed three distinct transitions, *i.e.* below pH 6, between pH 6.5 and 7, and above pH 7.5, respectively. The first and third transitions have tangent lines with slopes of +1 and −1, respectively. On the other hand, the curve for SM showed one large transition below pH 6 having a tangent line with a slope of +1, and no clear large transitions were observed in the alkaline pH region. This suggested that the curve for SM could be analyzed by assuming the participation of only two ionizable groups. Nevertheless, we analyzed the pH dependence data of k_{cat} for both the substrates on the same assumption for HNP that the three ionizable groups participate in the catalytic activity, since the catalytic mechanism should be common regardless of the substrate used. The ionizable group participating in the second transition in the pH dependence curve of k_{cat} was assigned to Asp 126, since the pH dependence curve of k_{cat} of D126G SMase showed no corresponding transition (Fujii *et al.*, to be published). Therefore, as the $pK^{EM_2SH_2}$ value required for analysis of this pH dependence curve of k_{cat} (Eq. 8 and Fig. 10), the pK value of the enzyme-Mg^{2+}-substrate complex (pK^{EM_2SH}) which had been determined from the pH dependence of $1/K_m$ (Eq. 7 and Fig. 9) was used.

The three-dimensional structures of none of the types of SMases has been solved yet. Recently, Matsuo *et al.* (*14*) predicted the three-dimensional structure of *B. cereus* SMase using a protein fold recognition method based on the structure of bovine pancreatic DNase I, which has the most compatible sequence with SMase and catalyzes the hydrolysis of phosphoester bonds like SMase. From the results of their X-ray crystallographic study, Weston *et al.* (*19*) proposed that His 252 of DNase I acts as a general base to accept a proton from a water molecule, which then, as a nucleophile, attacks the phosphoryl group; and His 134 functions as a general acid to protonate the leaving oxygen of the phosphoester. Sequence comparison revealed that His 252 and His 134 of bovine DNase I correspond to His 296 and His 151, respectively, in *B. cereus* SMase, which are conserved in all bacterial SMases (*14*). By site-directed mutagenesis, each of these two His residues of *B. cereus* SMase was substituted with Ala, and the hydrolytic activities of the resultant mutant SMases (H151A and H296A) toward SM and HNP as substrates were found to be extremely low in comparison with those of the wild-type SMase (*14*). These results suggested that the catalytic mechanism of *B. cereus* SMase comprises general-acid-base catalysis, and that His 296 and His 151 act as a general base and acid, respectively.

In the present study, the pH dependence curve of the logarithm of k_{cat} for the hydrolysis of HNP catalyzed by *B. cereus* SMase was shown to have tangent lines with slopes of +1 and −1 in the acid and alkaline pH ranges, respectively. This was in good agreement with the idea of general-acid-base catalysis. On the other hand, the curve for SM had a tangent line with a slope of +1 in the acid pH range and one of nearly 0 in the alkaline pH range, which does not agree with the idea of general-acid-base catalysis. Therefore, we proposed a catalytic mechanism for SMase based on general-base catalysis (Fig. 12).

On the basis of the predicted three-dimensional structure of this enzyme and on the present kinetic data, the ionizable group having $pK^{EM_2SH_2} = 5.85$ in Fig. 10 and Eq. 8 is assigned to His 296, which acts as a general-base. The ionizable group having $pK^{EM_2SH_1} = 7.60$ is not a true catalytic residue, but a very important residue for the catalytic activity toward HNP.

REFERENCES

1. Tomita, M., Taguchi, R., and Ikezawa, H. (1991) Sphingomyelinase of *Bacillus cereus* as a bacterial hemolysin. *J. Toxicol. Toxin Rev.* **10**, 169-207
2. Hannun, Y.A. (1994) The sphingomyelin cycle and the second messenger function of ceramide. *J. Biol. Chem.* **269**, 3125-3128
3. Liu, B., Obeid, L.M., and Hannun, Y.A. (1997) Sphingomyelinases in cell regulation. *Semin. Cell Dev. Biol.* **8**, 311-322
4. Quintern, L.E., Schuchman, E.H., Levran, O., Suchi, M., Ferlinz, K., Reinke, H., Sandhoff, K., and Desnick, R.J. (1989) Isolation of cDNA clones encoding human acid sphingomyelinase: occurrence of alternatively processed transcripts. *EMBO J.* **8**, 2469-2473
5. Tomiuk, S., Hofmann, K., Nix, M., Zumbansen, M., and Stoffel,

W. (1998) Cloned mammalian neutral sphingomyelinase: Functions in sphingolipid signalling? *Proc. Natl. Acad. Sci. USA* **95**, 3638-3643
6. Yamada, A., Tsukagoshi, N., Udaka, S., Sasaki, T., Makino, S., Nakamura, S., Little, C., Tomita, M., and Ikezawa, H. (1988) Nucleotide sequence and expression in *Escherichia coli* of the gene coding for sphingomyelinase of *Bacillus cereus*. *Eur. J. Biochem.* **175**, 213-220
7. Strum, J.C., Swenson, K.I., Turner, J.E., and Bell, R.M. (1995) Ceramide triggers meiotic cell cycle progression in *Xenopus* oocytes. A potential mediator of progesterone-induced maturation. *J. Biol. Chem.* **270**, 13541-13547
8. Tamura, H., Noto, M., Kinoshita, K., Ohkuma, S., and Ikezawa, H. (1994) Inhibition of NGF-induced neurite outgrowth of PC12 cells by *Bacillus cereus* sphingomyelinase, a bacterial hemolysin. *Toxicon* **32**, 629-633
9. Raines, M.A., Kolesnick, R.N., and Golde, D.W. (1993) Sphingomyelinase and ceramide activate mitogen-activated protein kinase in myeloid HL-60 cells. *J. Biol. Chem.* **268**, 14572-14575
10. Linardic, C.M. and Hannun, Y.A. (1994) Identification of a distinct pool of sphingomyelin involved in the sphingomyelin cycle. *J. Biol. Chem.* **269**, 23530-23537
11. Tomita, M., Ueda, Y., Tamura, H., Taguchi, R., and Ikezawa, H. (1993) The role of acidic amino-acid residues in catalytic and adsorptive sites of *Bacillus cereus* sphingomyelinase. *Biochim. Biophys. Acta* **1203**, 85-92
12. Tamura, H., Tameishi, K., Yamada, A., Tomita, M., Matsuo, Y., Nishikawa, K., and Ikezawa, H. (1995) Mutation in aspartic acid residues modifies catalytic and haemolytic activities of *Bacillus cereus* sphingomyelinase. *Biochem. J.* **309**, 757-764
13. Ikezawa, H., Tameishi, K., Yamada, A., Tamura, H., Tsukamoto, K., Matsuo, Y., and Nishikawa, K. (1995) Studies on the active sites of *Bacillus cereus* sphingomyelinase substitution of some amino acids by site-directed mutagenesis. *Amino Acids* **9**, 293-298
14. Matsuo, Y., Yamada, A., Tsukamoto, K., Tamura, H., Ikezawa, H., Nakamura, H., and Nishikawa, K. (1996) A distant evolutionary relationship between bacterial sphingomyelinase and mammalian DNase I. *Protein Sci.* **5**, 2459-2467
15. Tomita, M., Nakai, K., Yamada, A., Taguchi, R., and Ikezawa, H. (1990) Secondary structure of sphingomyelinase from *Bacillus cereus*. *J. Biochem.* **108**, 811-815
16. Wetlaufer, D.B. (1962) Ultraviolet spectra of proteins and amino acids in *Advances in Protein Chemistry* (Anfinsen, C.B., Jr., Anson, M.L., Bailey, K., and Edsall, J.T., eds.) Vol. 17, pp. 303-390, Academic Press, New York
17. Gal, A.E., Brady, R.O., Hibbert, S.R., and Pentchev, P.G. (1975) Practical chromogenic procedure for the detection of homozygotes and heterozygous carriers of Niemann-Pick disease. *N. Engl. J. Med.* **293**, 632-636
18. Ikeda, K., Inoue, S., Amasaki, C., Teshima, K., and Ikezawa, H. (1991) Kinetics of the hydrolysis of monodispersed and micellar phosphatidylcholines catalyzed by a phospholipase C from *Bacillus cereus*. *J. Biochem.* **110**, 88-95
19. Weston, S.A., Lahm, A., and Suck, D. (1992) X-ray structure of the DNase I-d(GGTATACC)$_2$ complex at 2.3 Å resolution. *J. Mol. Biol.* **226**, 1237-1256